Hydroisomerization of *n*-hexane over Pt-ETS-10

Tapan Kr. Das, A.J. Chandwadkar, H.S. Soni and S. Sivasanker *

National Chemical Laboratory, Pune 411008, India

Received 4 September 1996; accepted 9 December 1996

The hydroisomerization of *n*-hexane has been investigated at atmospheric pressure in the temperature range 523–623 K over Pt-H-ETS-10 containing different amounts of Pt. The influence of Pt content and reaction parameters on the isomerization efficiency is reported. The optimum Pt content for the reaction was found to be around 0.3% Pt. The moderate acidity of the molecular sieve (H-form) results in high selectivities for isomerization. The studies suggest that *n*-hexane transformation over Pt-H-ETS-10 proceeds through a bifunctional route.

Keywords: hydroisomerization, *n*-hexane hydroisomerization, molecular sieves, ETS-10, titanosilicates

1. Introduction

Catalytic hydroisomerization of light naphtha (C_5–C_6 fraction) is practiced in many refineries to increase the gasoline pool octane [1,2]. The process essentially transforms the low-octane components such as the *n*-paraffins into high-octane branched chain components with minimal cracking. Highly acidic zeolites and silica alumina containing small amounts of a noble metal such as Pt have been reported to be suitable catalysts [3]. The hydroisomerization of model compounds such as *n*-hexane and *n*-heptane has been reported over large number of zeolites and aluminophosphate catalysts containing Pt [4–6].

We now report our studies on the hydroisomerization of *n*-hexane over a moderately acidic wide-pore titanosilicate, ETS-10, containing a small amount of Pt. ETS-10 has a unique molecular architecture arising from the octahedrally co-ordinated framework Ti^{4+} ions (unlike in normal zeolites, in which all the ions are in tetrahedral co-ordination in the framework). ETS-10 has an open three-dimensional structure consisting of Ti^{4+} octahedral chains linked to classical tetrahedral silica rings [7] resulting in a pore system of ~ 8 Å diameter. By virtue of the Ti^{4+} (O_h) ions being attached to Si^{4+} (T_d) ions, there is an excess negative charge of two units per Ti-ion requiring neutralization by two monovalent ions. When the charge-balancing ions are protons, the molecular sieve is moderately acidic.

2. Experimental

ETS-10 samples were prepared following the reported procedure [8]. The sample was characterized by XRD, SEM, IR and adsorption studies. The XRD pattern of the sample is similar to that reported earlier. Scanning electron micrographs revealed an almost uniform particle size of ~ 1 μm. The adsorption capacity for the different probe molecules, namely, water, *n*-hexane and trimethylbenzene (at 25°C and $p/p_0 = 0.5$) were 17.0, 12.1 and 11.2 wt%, respectively. The BET surface area of the sample (N_2-adsorption) was 410 m^2/g. The sample was converted into the protonic form by exchanging thrice with an ammonium nitrate solution (20 ml of 1 M solution/g of catalyst at 373 K for 10 h), filtered, washed, dried at 383 K and calcined at 648 K for 5 h. The chemical composition of the protonic form of the sample in terms of the oxides was as follows: $0.23Na_2O : 0.033K_2O : TiO_2 : 5.10SiO_2 : 2.90H_2O$.

The metal loading of H-ETS-10 was carried out by wet impregnation with tetraamine platinum(II) nitrate (Aldrich, 99% purity) to get Pt-loadings of 0.1, 0.2, 0.3, 0.4 and 0.5 wt%. After impregnation the materials were dried in air at 383 K for 4 h and finally calcined at 623 K for 3 h in air and reduced at 648 K for 4 h in hydrogen.

Temperature-programmed desorption of NH_3 studies on H-ETS-10 and Pt-H-ETS-10 were carried out following a procedure described earlier [9].

The catalytic reactions were carried out in a down-flow fixed-bed glass reactor (i.d. = 15 mm) at atmospheric pressure using about 2 g of the catalyst. The catalyst was compacted in a hydraulic press and broken into small pieces (16–20 mesh) prior to use. *n*-hexane was $> 99\%$ pure (S.D. Fine Chemicals Pvt. Ltd., Bombay). Analysis of both the gaseous and liquid products was carried out by gas chromatography (HP 5880) using a capillary column (cross-linked methyl silicone gum, HP1, 50 m × 0.2 mm i.d.; detector, FID).

3. Results and discussion

The profiles of temperature-programmed desorption of NH_3 obtained over H-ETS-10 and Pt-H-ETS-10 are

* To whom correspondence should be addressed.

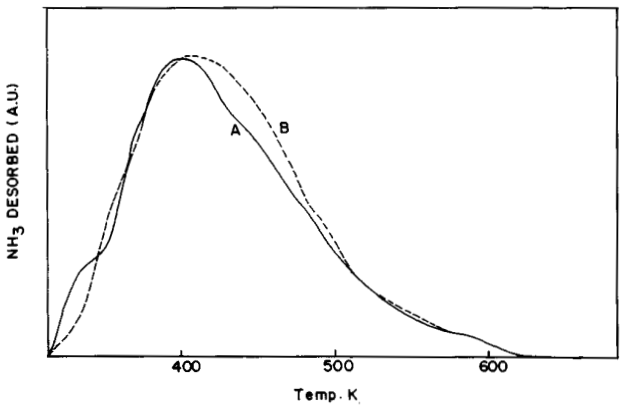

Fig. 1. Temperature-programmed desorption of NH_3. (A) H-ETS-10; (B) Pt(0.3 wt%)-H-ETS-10.

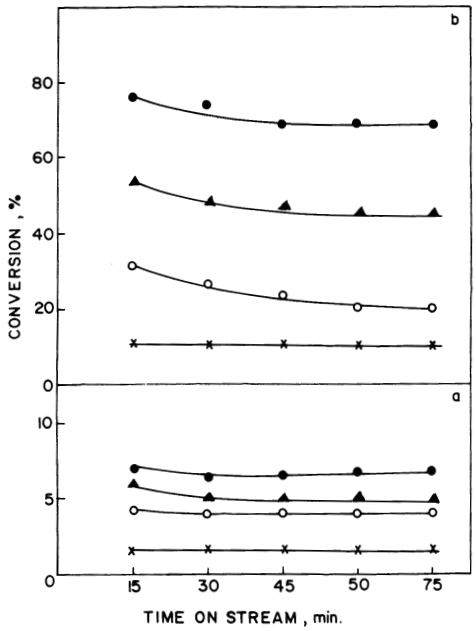

Fig. 2. Effect of temperature and Pt-content on catalyst deactivation with duration of run (time on stream = TOS). WHSV (h^{-1}) = 1.0; H_2/*n*-hexane (mole) = 4.5; (×) 523 K; (○) 573 K; (▲) 598 K and (●) 623 K. (a) H-ETS-10; (b) Pt (0.3 wt%)-H-ETS-10.

presented in fig. 1. The profiles indicate that the acid sites are mostly of weak to moderate strength. For example, nearly all the NH_3 is desorbed below 623 K, the peak maximum occurring around 400–420 K. In comparison, strongly acidic zeolites such as H-ZSM-5 continue to desorb NH_3 beyond 733 K with a distinct peak maximum for strong acid sites occurring around 670 K [10]. Pt-dispersion measurements were carried out on a 0.5 wt% sample by H_2 adsorption at ambient temperature [11]. A Pt-dispersion of about 72% was estimated. The above value is probably low as the degassing of the reduced sample was done at the relatively low temperature of 598 K to prevent structural damage to ETS-10.

The incorporation of Pt increases the activity of ETS-10 many-fold, being about five-fold at 523 K and eight-fold at 623 K (fig. 2). Fig. 2 also reveals that a decrease in *n*-hexane conversion occurs with duration of run, the decrease being generally more at higher temperatures than at lower temperatures. The decrease, however, is not noticeable beyond about 30 min. The data reported in the rest of the paper were, hence, collected at a time on stream (TOS) of 45 min.

3.1. Influence of Pt-content

The transformation of *n*-hexane was carried out at atmospheric pressure in the temperature range of 473 to 573 K over Pt-ETS-10 samples containing different amounts of Pt (0.1–0.5 wt%). The conversion increases with increasing Pt-content at all the temperatures studied (473–573 K) and reaches a nearly constant value beyond 0.3% Pt (fig. 3a). The above observation is typical of bifunctional catalysis [12–14]. A similar constant conversion beyond 0.5% Pt has also been reported by earlier workers [15] in the case of Pt-HY.

The influence of Pt-content on selectivity to isomerization expressed as the isomerization/cracking ratio (I/C) is depicted in fig. 3b. The I/C ratio increases with Pt content and reaches a maximum at about 0.3 wt% Pt. Alvarez et al. [16] have reported a similar maximum at 1.0 wt% Pt during their studies on a Pt-H-Y (Si/Al = 9) catalyst. An examination of the distribution of the isohexane in the product (at 598 K; fig. 3c) reveals that the distribution is altered by the addition of Pt. However, the distribution is similar when the Pt content is 0.3% or more. This is also evident from the ratio of the different hexane isomers (fig. 3d). The 2-methylpentane/3-methylpentane ratio (2-MP/3-MP) is close to the equilibrium value of 1.57 [14] when the Pt content is 0.3% or more. When Pt is absent (H-ETS-10), the ratio is 1.27. Again, the 2,3-dimethylbutane/2,2-dimethylbutane ratio (2,3-DMB/2,2-DMB) is about 3.6 in Pt-ETS-10 samples and 6.8 in H-ETS-10, much farther from the equilibrium value of 0.86. The conclusions are that the incorporation of Pt greatly enhances the isomerization activity besides assisting the interconversions of the isomeric hexanes.

3.2. Influence of temperature

The influence of temperature on the reaction is presented in fig. 4. *n*-hexane conversion increases with temperature, the increase being more marked beyond 573 K and at higher Pt-contents (fig. 4a). The I/C ratio on the other hand, interestingly, goes through a maximum for all the catalysts (with different Pt-contents; fig. 4b). Earlier workers have, however, reported a continuous decrease in the I/C ratio with temperature [17]. The reason for the maximum over the Pt-H-ETS-10 catalysts is not clear, though a possible explanation is that at moder-

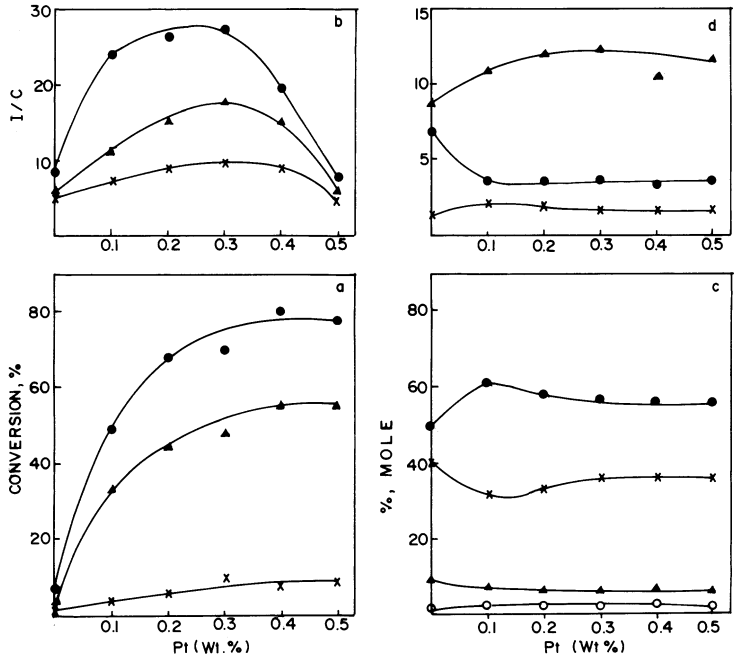

Fig. 3. Influence of Pt-content on *n*-hexane isomerization. Catalyst, Pt(0.3 wt%)-H-ETS-10; WHSV (h^{-1}) = 1.0; H_2/*n*-hexane (mole) = 4.5; TOS = 45 min. (a) (×) 523 K; (▲) 598 K and (●) 623 K. (b) (×) 523 K; (▲) 573 K and (●) 598 K. (c) Temp. = 598 K; (○) 2,2-DMB; (▲) 2,3-DMB; (×) 3-MP and (●) 2-MP. (d) Temp. = 598 K; (×) 2-MP/3-MP; (●) 2,3-DMB/2,2-DMB and (▲) MP/DMB.

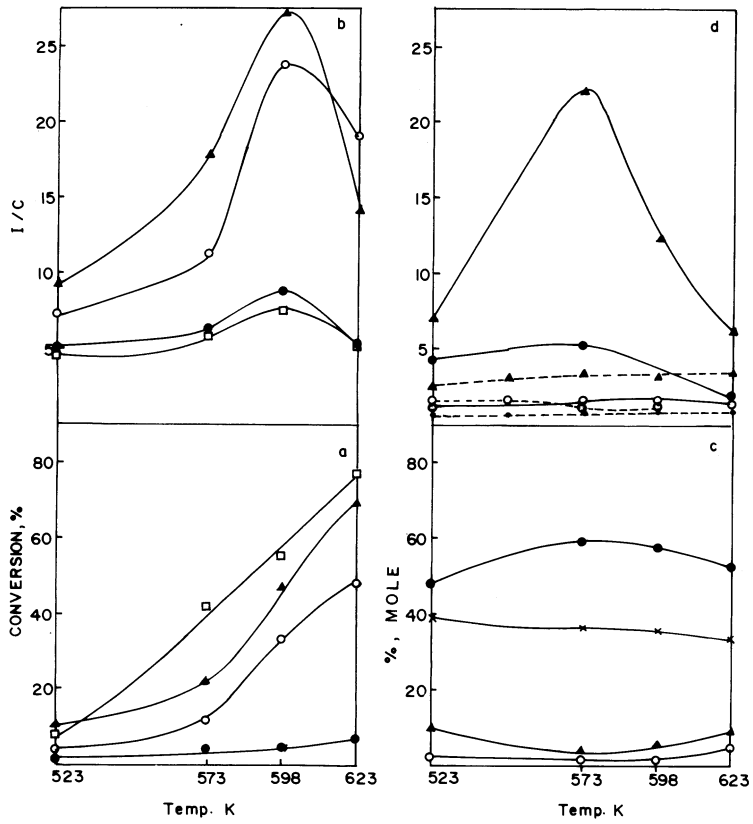

Fig. 4. Influence of temperature on isomerization of *n*-hexane. WHSV (h^{-1}) = 1.0; H_2/*n*-hexane (mole) = 4.5; TOS = 45 min. (a,b) (●) H-ETS-10; (○) Pt(0.1 wt%)-H-ETS-10; (▲) Pt (0.3 wt%)-H-ETS-10 and (□) Pt (0.5 wt%)-H-ETS-10. (c) Catalyst, Pt (0.3 wt%)-H-ETS-10; (○) 2,2-DMB; (▲) 2,3-DMB; (×) 3-MP and (●) 2-MP. (d) Catalyst, Pt (0.3 wt%)-H-ETS-10; (●) 2,3-DMB/2,2-DMB; (○) 2-MP/3-MP and (▲) MP/DMB; (——) experimental data and (- - -) thermodynamic data.

ate temperatures (598 K), the desorption of the intermediate iso-olefin and its migration to the metal sites to undergo hydrogenation into stable isoparaffins is maximum. At the still higher temperature of 623 K, hydrogenolysis activity by the metal sites becomes more, thereby lowering the I/C ratio. This is suggested by the lower I/C values for the 0.5% Pt catalyst than for the 0.3% Pt catalyst (fig. 4b). The concentration of 2-methylpentane goes through a maximum at an intermediate temperature while those of the dibranched isomers increase (fig. 4c). The decrease in the concentrations of the monobranched isomers is due to their undergoing isomerization into the dibranched isomers and cracking into C_1–C_5 products at higher temperatures. The 2-MP/3-MP ratios are close to the equilibrium value of 1.57 at all the temperatures (fig. 4d). The 2,3-DMB/2,2-DMB ratio and mono-/di-branched (M/D) ratios are, however, far from the equilibrium ratios, though there is a tendency for the ratios to approach the equilibrium values. Interestingly, the M/D ratios also go through a maximum at intermediate temperatures.

3.3. Influence of space velocity

Increasing the contact time (1/WHSV) increases conversion and decreases the I/C ratios (fig. 5a). The decrease in I/C ratios is probably mainly due to an increase in cracking, which being slower than the isomerization reactions are favoured at larger residence times. Besides, at these conditions, larger concentrations of the more easily cracked isomerized products (secondary and tertiary carbocations) are present. A 2-MP/3-MP ratio of 1.62 ± 0.06 is observed in the WHSV range studied. This is close to the equilibrium value of 1.57 [13]. However, the 2,3-DMB/2,2-DMB and M/D ratios are farther away from the equilibrium ratios at low contact times and tend to approach the equilibrium values at higher contact times (fig. 5b). These observations suggest that the sequence of *n*-hexane isomerization reactions is as shown:

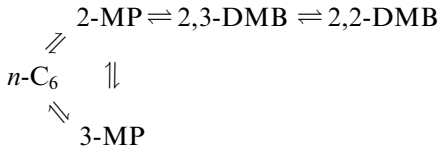

The above sequence has already been suggested by earlier workers [12,13]. The ratios of the different products also suggest that the isomerization of 2,3-DMB to 2,2-DMB is the most difficult step. McCaulay [18] has reported that it is indeed so; he has found that the relative rates of isomerization of the different hexane isomers over HF/BF_3 are as follows: 2-MP to 3-MP $= 58 \times 10^3$; MP to DMB = 58; 2,3-DMB to 2,2-DMB = 8.6. The low yields of the dibranched isomers over the Pt-ETS-10 samples is probably due to the absence of strong acidity necessary to carry out the difficult mono- to di-branched isomer transformations.

3.4. Influence of H_2/n-C_6 (mole) ratio

The influence of H_2/n-C_6 mole ratio is presented in table 1. Increasing the *n*-hexane mole ratio from 4.5 to 15 (at constant feed rate of *n*-C_6) decreases the conversion. The decrease is probably due to an increase in total ($H_2 + n$-C_6) space velocity and due to a negative (or lower) order with respect to H_2. Earlier workers have reported reaction orders of 0 to 0.3 with respect to *n*-C_6 and 0.3 to -0.6 with respect to H_2 for the hydroisomerization of *n*-C_6 over Pt-mordenite [4]. As the hydrogen partial pressure change was only $\sim$ 13% (0.82–0.93), the larger change in conversion ($\sim$ 27%) from 47.4 to 34.5 suggests that the decrease in conversion is due to both the reasons mentioned above.

4. Conclusions

The hydroisomerization of *n*-hexane occurs over Pt-H-ETS-10 with high selectivities due to moderate acidity

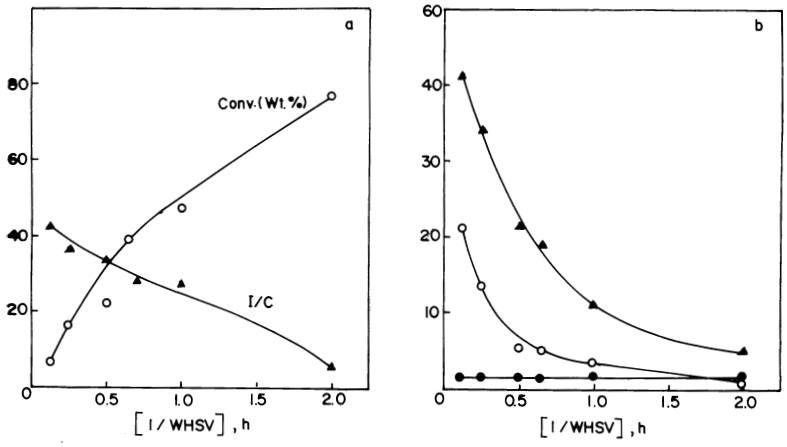

Fig. 5. Influence of space velocity on *n*-hexane isomerization. Catalyst, Pt(0.3 wt%)-H-ETS-10; temp. = 598 K; H_2/n-hexane (mole) = 4.5; TOS = 45min. (b) (●) 2-MP/3-MP; (○) 2,3-DMB/2,2-DMB and (▲) MP/DMB.

Table 1
Influence of H_2/*n*-hexane (mole) ratio on the product distribution [a]

	H_2/*n*-hexane (mole ratio)		
	4.5	10.0	15.0
conversion (%)	47.4	40.9	34.5
I/C [b] ratio	26.8	32.8	37.1
products (wt%)			
C_1–C_5	1.7	1.2	0.9
2-MP	25.6	23.4	20.1
3-MP	15.9	13.1	10.2
2,3-DMB	2.6	1.9	2.1
2,2-DMB	0.8	0.6	0.6
methylcyclopentane	0.7	0.4	0.4
C_6 + aliphatics	0.1	0.3	0.2
2-MP/3-MP	1.6	1.8	2.0
MP/DMB	12.2	14.6	11.2
2,3-DMB/2,2-DMB	3.3	3.2	3.5

[a] Reaction conditions: catalyst, Pt(0.3 wt%)-H-ETS-10; temp. = 598 K; WHSV (h^{-1}) = 1.0; pressure = 1 atm; TOS = 45 min.
[b] I/C = isomerization (including methylcyclopentane)/cracking.

of the material. The isomerization selectivity is maximum at around 0.3 wt% Pt in the catalyst and at around 600 K. Though the yields of methylpentanes are in near equilibrium amounts, the di-methyl isomers are produced in low yields.

Acknowledgement

TKD thanks CSIR, New Delhi, for a research fellowship.

References

[1] N.A. Cusher, P. Greenouch, J.R.K. Rolfe and J.A. Weiszmann, in: *Handbook of Petroleum Refining Process*, ed. R.A. Meyers (McGraw-Hill, New York, 1986) ch. 5, p. 51.
[2] H.W. Kouwenhoven, in: *Molecular Sieves,* Adv. Chem. Ser., Vol. 121, eds. W.M. Mier and J.B. Uytterhoeven (Am. Chem. Soc., Washington, 1973) p. 529.
[3] R.B. La Pierre and R.D. Partridge, Eur. Patent Appl. 94827 (1983).
[4] M. Guisnet, V. Fouche, M. Belloum, J.P. Bournonville and C. Travers, Appl. Catal. 71 (1991) 295.
[5] L.J. Leu, L.Y. Hou, B.C. Kang, C. Li, S.-T. Wu and J.C. Wu, Appl. Catal. 69 (1991) 49.
[6] J.M. Campelo, F. Lafont and J.M. Marinas, Zeolites 15 (1995) 97.
[7] M.W. Anderson, O. Tarasaki, T. Ohsuma, A. Phillippou, S.P. Mackay, A. Ferreira, J. Rocha and Lidin, Nature 367 (1994) 347.
[8] T.K. Das, A.J. Chandwadkar and S. Sivasanker, J. Chem. Soc. Chem. Commun. (1996) 1105.
[9] J. Zheng, J.-L. Dong, Q.-H. Xu, Y. Liu and A.-Z. Yan, Appl. Catal. 126 (1995) 141.
[10] P. Ratnassamy, R.B. Borade, S. Sivasanker, V.P. Shiralkar and S.G. Hegde, Acta Phys. Chem. 31 (1985) 137.
[11] P.G. Smirniotis and E. Ruckenstein, Appl. Catal. 123 (1995) 59.
[12] P.B. Weisz, Adv. Catal. 13 (1962) 137.
[13] P.A. Jacobs, J.B. Uytterhoeven, M. Steijns, G. Foment and J. Weitkamp, in: *Proc. 5th Int. Conf. on Zeolites*, Naples, ed. L.V.C. Rees (Heyden, London, 1980) p. 607.
[14] J.-K. Chen, A.M. Martin, Y.G. Kim and V.T. John, Ind. Eng. Res. 27 (1988) 401.
[15] G.E. Giannetto, G.R. Pérot and M.R. Guisnet, Ind. Eng. Chem. Prod. Res. Dev. 25 (1986) 481.
[16] F. Alvarez, G. Gianetto, M. Guisnet and G. Pérot, Appl. Catal. 34 (1987) 353.
[17] R. Ravishankar and S. Sivasanker, Appl. Catal. 142 (1996) 47.
[18] D.A. McCaulay, J. Am. Chem. Soc. 84 (1959) 6437.